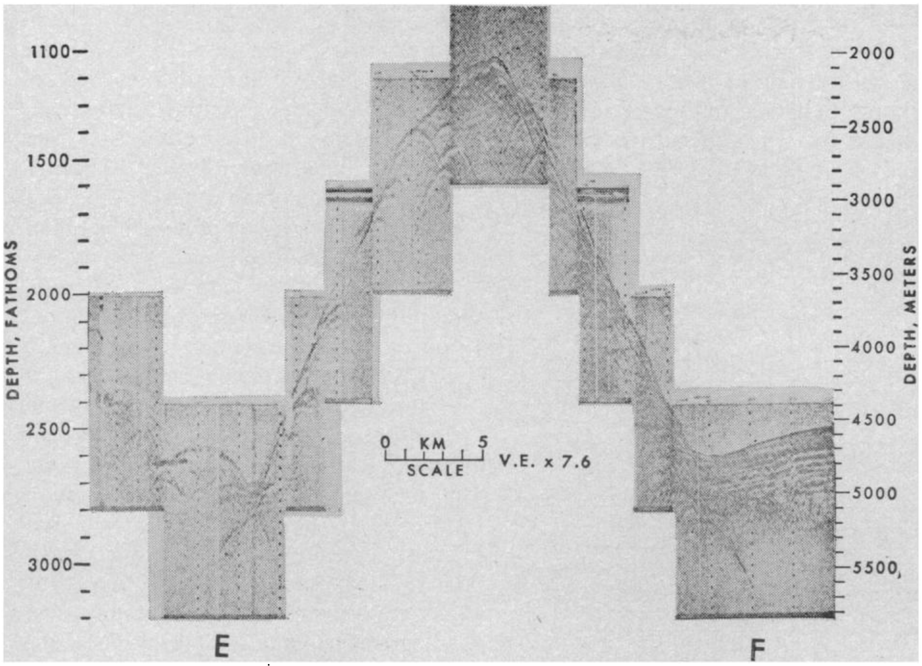

Fig. 3. A continuous seismic-reflection profile across Kodiak Seamount.

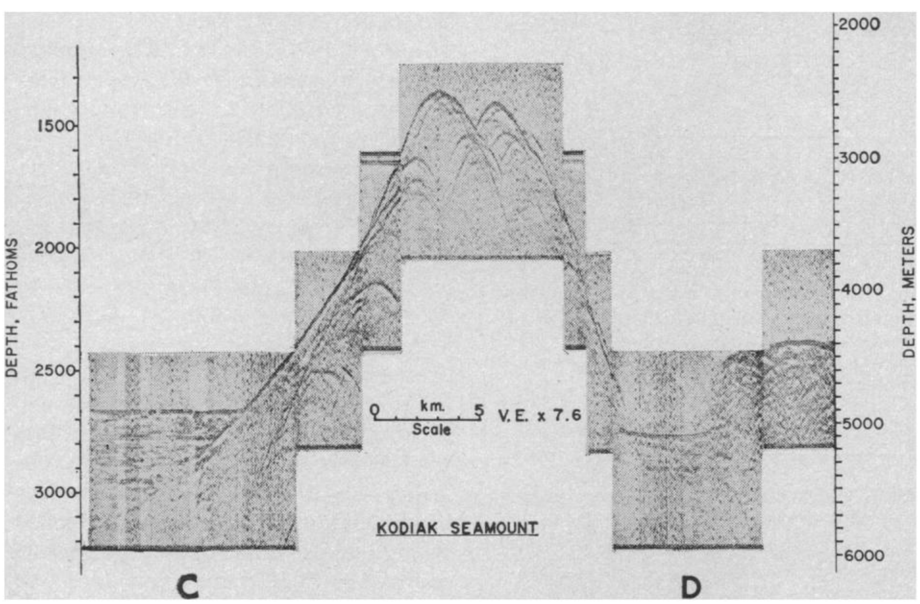

Fig. 4. Seismic-reflection profile across Kodiak Seamount. Faint reflections at *C* have been made darker by tracing over them with a pencil.

formed sediment that laps against the buried surface of the seamount. This indicates that the sediment was deposited after formation of the seamount.

Sediment moving past Kodiak Seamount to the southwest is apparently not deposited as quickly near the base of the seamount as it is deposited a relatively short distance away. Consequently, there is a small trough, or moat, formed on the south and southwest sides (Figs. 1 and 3, *F*). This trough is clearly shown in these figures to be a depositional feature, probably due to a scouring effect, or a slower rate of deposition because of accelerated turbidity currents around the seamount. The same effect is seen elsewhere on the abyssal plains to the south.

The parallel sub-bottom layers tilted toward and abutting the rock of the seamount are shown with no depositional moating effect. Overlying these layers are sediments forming the present curved surface of the sea floor, and the depositional moat or trough. Probably these lower beds were originally horizontal, and were tilted by regional warping or downbowing of the trench. Thus, the present depositional trough overlies an older tectonic trough. Large-scale tilting and subsequent sedimentation has been seen in continuous seismic-reflection profiles across the Aleutian Trench, both northwest and southeast of Kodiak Seamount.

E. L. HAMILTON
U.S. Navy Electronics Laboratory, San Diego, California

R. E. VON HUENE
U.S. Naval Ordnance Test Station, China Lake, California

References and Notes

1. H. W. Menard and R. S. Dietz, *Bull. Geol. Soc. Amer.* **62**, 1263 (1951).
2. H. H. Hess, *Amer. J. Sci.* **244**, 772 (1946); E. L. Hamilton, *Geol. Soc. Amer. Mem.* **64**, (1956).
3. The seismic-reflection profiling system utilized a modified Rayflex receiving and signal-processing system which triggered an electric arc discharge of up to 20 kilojoules from a Rayflex capacitor bank, and up to 18 kilojoules from an EGG capacitor bank.
4. R. J. Hurley, *Scripps Inst. Ref. 60-7* (1960).

21 September 1966

Air-Sea Waves from the Explosion of Krakatoa

Abstract. *The distant sea disturbances which followed the explosion of Krakatoa are correlated with recently discovered atmospheric acoustic and gravity modes having the same phase velocity as long waves on the ocean. The atmospheric waves jumped over the land barriers and reexcited the sea waves with amplitudes exceeding the hydrostatic values. An explosion of 100 to 150 megatons would be required to duplicate the Krakatoa atmospheric-pressure pulse.*

The explosion of the volcano Krakatoa in 1883 is remarkable in many respects. In magnitude it was probably the greatest explosion ever recorded. The atmospheric disturbance was detected by barographs at many stations throughout the world on at least three passages around the earth. Sea-level disturbances were observed on tide gages as far away as ports of the English Channel. The various phenomena and original data associated with the explosion have been documented in a report of a committee of the Royal Society (*1*).

A selection of tide-gage records redrawn from Symons (*1*) shows the sea-level disturbance at several distant stations (Fig. 1). Although the explosion produced one of the most destructive tidal waves on record, most investigators attributed the distant sea waves to disturbances which had no connection with the Krakatoa tsunami (*2*). They were forced to this conclusion because circuitous and highly improbable all-water propagation paths were required to avoid land barriers. In addition, the wave velocities for these paths were much higher than those derived by use of $\sqrt{gH}$ and the known depths of the ocean.

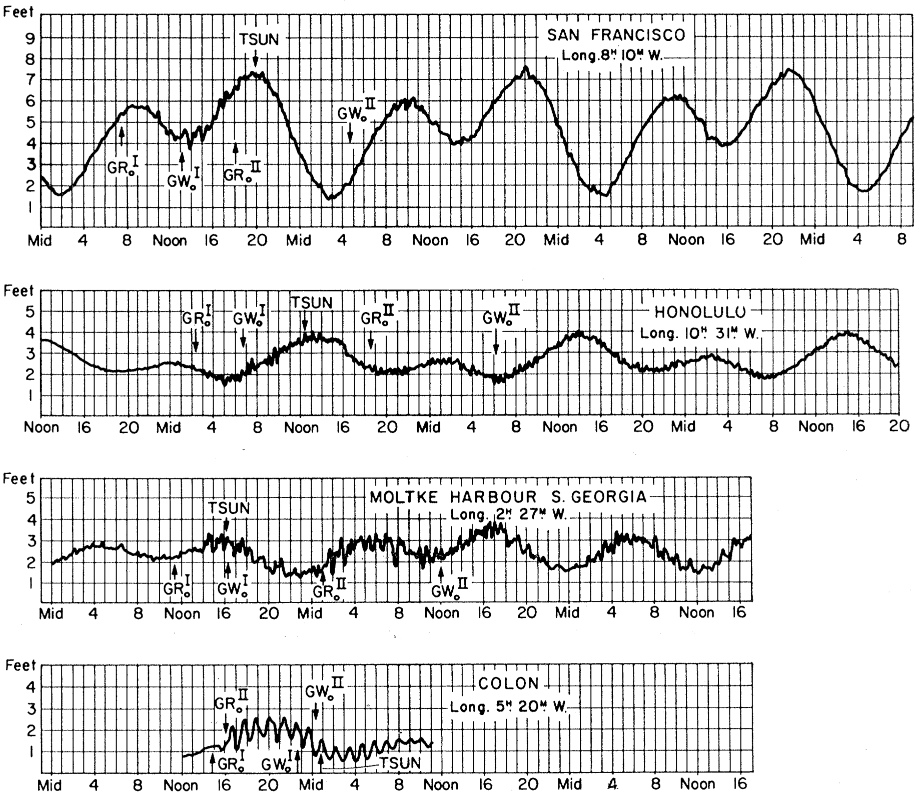

Fig. 1. Marigrams for San Francisco, Honolulu, South Georgia, and Colon. Arrows indicate theoretical arrival times of several modes and the tsunami. Roman superscripts indicate short (I) and long (II) great-circle paths. Abscissa is local civil time beginning 27 August 1883. (The exception is Honolulu which begins 26 August.)

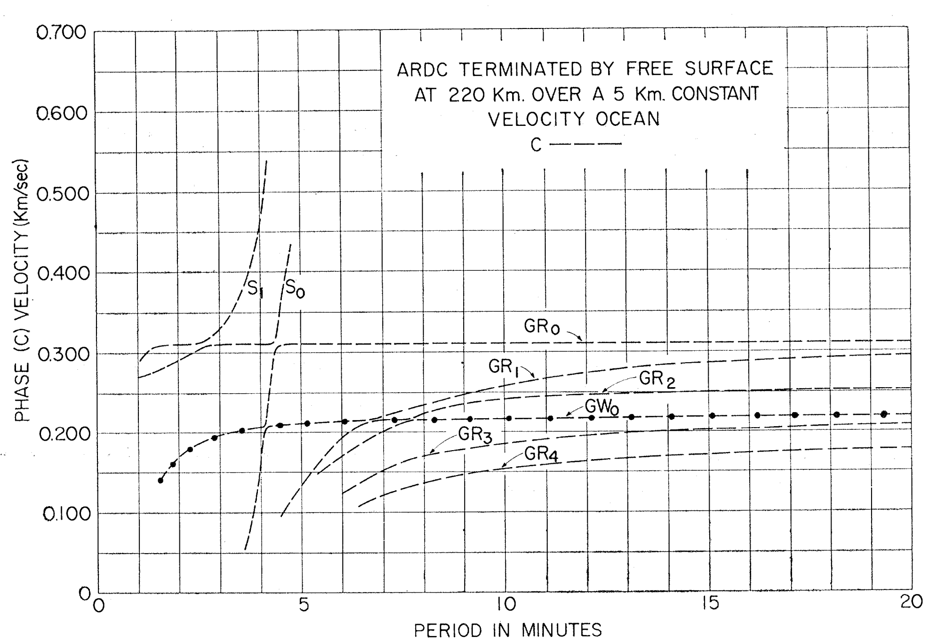

Fig. 2. Phase-velocity dispersion curves for modes of a standard ARDC atmosphere underlain by an ocean with a depth of 5 km.

Ewing and Press (*2*) noted the nearly coincident arrival of the atmospheric pulse (traveling in the direction from continent to ocean) and sea waves, and proposed that the latter were excited by the former. The sea disturbance was much greater than could be accounted for by the hydrostatic effect of the atmospheric pulse, requiring some mechanism of amplification or resonance. Ewing and Press (*2*) suggested that resonant coupling might be the mechanism if free waves in the atmosphere existed with velocities near 220 m/sec, the velocity of $\sqrt{gH}$ waves in the deep ocean. Their explanation suffered in that such waves were not known theoretically or experimentally.

We have extended the theoretical and numerical techniques developed for the study of internal acoustic-gravity waves generated by explosions in the atmosphere (*3*) to include the case where the bottom layer is an ocean with a depth of 5 km. The method involves approximating the known temperature variation in the atmosphere by a large number of isothermal layers. The results show that free waves in the atmosphere do exist with phase velocities near the $\sqrt{gH}$ velocity of the ocean. This leads to an efficient transfer of energy from the atmosphere to the ocean, and produces sea waves with amplitudes several times larger than hydrostatic.

Phase-velocity curves for the atmosphere-ocean system are shown in Fig. 2. The curve formed by connecting the dots is that of long gravity waves in the ocean (GW_0) in the absence of an atmosphere. At long periods it approaches $\sqrt{gH}$ asymptotically. All the other curves correspond to internal acoustic (S) or gravity (GR) modes in an atmosphere without an ocean. It is seen that the atmospheric modes GR_0, GR_1, GR_2, and GR_3 all have phase velocities which cross the GW_0 mode when the atmosphere and ocean are considered separately. In the combined atmosphere-ocean system, mode crossing does not occur, but the curves turn sharply and join the mode they would have crossed. In the coupled system, the GW_0 mode consists of segments of several modes.

Thus, the purely ocean mode is present in the coupled system and should be excited by an atmospheric source, essentially by the atmospheric modes

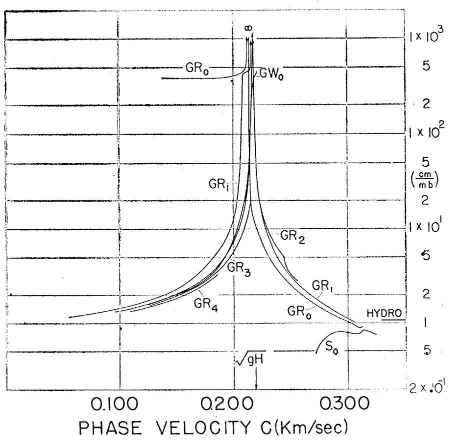

Fig. 3. Dynamic ratio of sea-surface displacement to pressure as a function of phase velocity.

with the same phase velocity. That this is the case is shown in Fig. 3 where the ratio of ocean displacement to atmospheric pressure at sea level is plotted as a function of phase velocity. Resonant peaks are found in all the gravity modes, the ratio being at least ten times greater than the hydrostatic value for the phase-velocity range of 195 to 230 m/sec. Thus amplitude build-up of the sea waves should begin before the arrival of the GW_0 group.

These results may be combined by Fourier synthesis to form a synthetic time series of sea-level displacement and atmospheric pressure as in Fig. 4. The first pressure pulse corresponds to the GR_0 mode and the accompanying sea wave is essentially the hydrostatic response. The main sea waves are in the GW_0 mode and propagate along great-circle paths with phase velocity near $\sqrt{gH}$. These are excited so efficiently by atmospheric waves with the same phase velocity that no corresponding large motion is shown on the pressure record. Intervening land barriers are jumped by the air waves which reexcite the sea wave if a sufficiently long fetch is available.

The theoretical group arrival times for the several modes and tsunami are shown in the tide-gage records of Fig. 1. It is seen that the sea waves begin and then reach large amplitudes in the interval between the GR_0 and GW_0 arrival times, as expected from the theory. The theoretical tsunami arrival times are too late, and the paths are improbable for San Francisco, Honolulu, and Colon. South Georgia may have received direct tsunami waves. Colon shows large amplitudes beginning just after GR_0 and continuing through GW_0. Its position near the antipodes, where the GR_0 waves are especially reinforced, may account for this. In view of the uncertain response of the instruments and the possibility of harbor resonances, no attempt was made to account for the absolute height or the spectrum of the sea waves.

Harkrider (*3*) showed how the properties of the source can be recovered from the pressure record. Using his scaling method, and data from nuclear explosions, we estimate that a surface explosion amounting to about 100 to 150 megatons would produce pressure pulses equivalent to those observed from Krakatoa.

FRANK PRESS

Department of Geology and Geophysics, Massachusetts Institute of Technology, Cambridge

DAVID HARKRIDER

Department of Geological Sciences, Brown University, Providence, Rhode Island

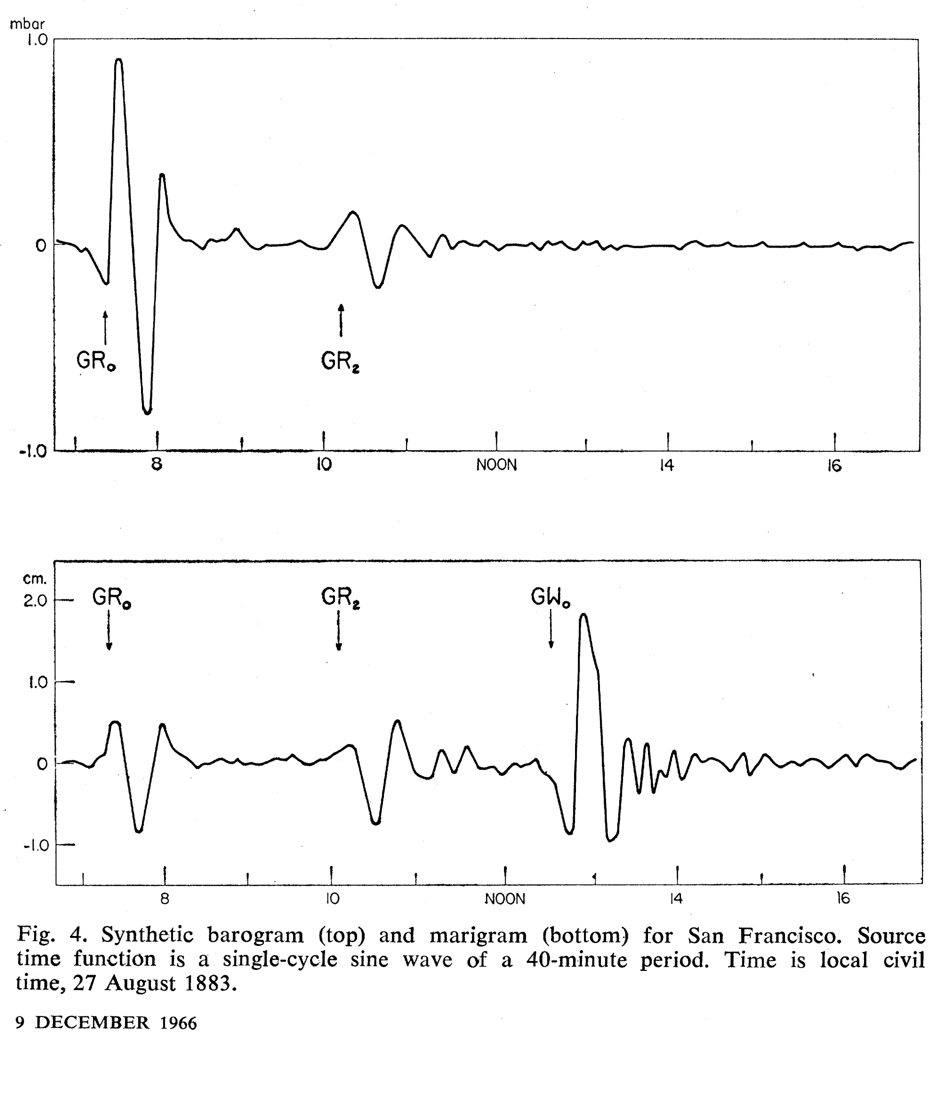

Fig. 4. Synthetic barogram (top) and marigram (bottom) for San Francisco. Source time function is a single-cycle sine wave of a 40-minute period. Time is local civil time, 27 August 1883.

References and Notes

1. G. J. Symons, Ed., *The Eruption of Krakatoa and Subsequent Phenomena* (Trubner, London, 1888).
2. M. Ewing and F. Press, *Trans. Amer. Geophys. Union* **36**, 53 (1955).
3. F. Press and D. Harkrider, *J. Geophys. Res.* **67**, 3889 (1962); D. Harkrider, *ibid.* **69**, 5295 (1964).
4. Supported by ARPA and monitored by AFO contracts AF 49(638)-1632 and AF 49(638)-1693.

26 August 1966

Reversible Inactivation of Aged Solutions of Indolyl-3-Acetic Acid

Abstract. Aqueous solutions of indole-3-acetic acid are inactivated by standing for a variable period of time. Inactivation results from conversion by oxidation of the plant hormone to polymerized deuterauxin, which is depolymerized by boiling of the solution, which restores activity.

Aqueous solutions of indole-3-acetic acid (IAA)—one of the most important plant hormones (auxins)—at physiological concentrations, say 5 μM, are completely inactivated, as tested by the coleoptile cylinder bioassay (*1*), after a variable length of time. In our laboratory, complete inactivation may occur after a period of 24 to 48 hours. Figure 1 illustrates the results of two